AFRL-RB-WP-TM-2010-3001

ANALYSIS OF MODAL GROWTH ON THE LEEWARD CENTERPLANE OF THE X-51 VEHICLE

Graham Candler, Heath Johnson, Christopher Alba, and Matthew MacLean

University of Minnesota

SEPTEMBER 2009
Final Report

AIR FORCE RESEARCH LABORATORY
AIR VEHICLES DIRECTORATE
WRIGHT-PATTERSON AIR FORCE BASE, OH 45433-7542
AIR FORCE MATERIEL COMMAND
UNITED STATES AIR FORCE

NOTICE AND SIGNATURE PAGE

Using Government drawings, specifications, or other data included in this document for any purpose other than Government procurement does not in any way obligate the U.S. Government. The fact that the Government formulated or supplied the drawings, specifications, or other data does not license the holder or any other person or corporation; or convey any rights or permission to manufacture, use, or sell any patented invention that may relate to them.

This report was cleared for public release by the USAF 88th Air Base Wing (88 ABW) Public Affairs Office (PAO) and is available to the general public, including foreign nationals. Copies may be obtained from the Defense Technical Information Center (DTIC) (http://www.dtic.mil).

AFRL-RB-WP-TM-2010-3001 HAS BEEN REVIEWED AND IS APPROVED FOR PUBLICATION IN ACCORDANCE WITH THE ASSIGNED DISTRIBUTION STATEMENT.

*//Signature//

ALYSON TURRI
Project Engineer
Aerodynamic Configuration Branch
Aeronautical Sciences Division

//Signature//

CHRISTOPHER P. GREEK
Chief
Aerodynamic Configuration Branch
Aeronautical Sciences Division

//Signature//

Dr. CARL P. TILMANN
Technical Advisor
Aerodynamic Configuration Branch
Aeronautical Sciences Division

This report is published in the interest of scientific and technical information exchange and its publication does not constitute the Government's approval or disapproval of its ideas or findings.

*Disseminated copies will show "//Signature//" stamped or typed above the signature blocks.

REPORT DOCUMENTATION PAGE

Form Approved
OMB No. 0704-0188

1. REPORT DATE *(DD-MM-YY)*	2. REPORT TYPE	3. DATES COVERED *(From - To)*
September 2009	Final	01 October 2008 – 30 August 2009

4. TITLE AND SUBTITLE
ANALYSIS OF MODAL GROWTH ON THE LEEWARD CENTERPLANE OF THE X-51 VEHICLE

5a. CONTRACT NUMBER
FA9550-04-1-0341

5b. GRANT NUMBER

5c. PROGRAM ELEMENT NUMBER
0602201

6. AUTHOR(S)
Graham Candler and Heath Johnson (University of Minnesota)
Christopher Alba (AFRL/RBAA)
Matthew MacLean (Calspan-University of Buffalo Research Center)

5d. PROJECT NUMBER
A0EF

5e. TASK NUMBER

5f. WORK UNIT NUMBER
0A

7. PERFORMING ORGANIZATION NAME(S) AND ADDRESS(ES)

University of Minnesota
117 Pleasant Street
Minneapolis, MN 55455

Calspan-University of Buffalo Research Center (CUBRC)
4455 Genesee Street
Buffalo, NY 14225

Aerodynamic Configuration Branch (AFRL/RBAA)
Control Sciences Division
Air Force Research Laboratory, Air Vehicles Directorate
Wright-Patterson Air Force Base, OH 45433-7542
Air Force Materiel Command, United States Air Force

8. PERFORMING ORGANIZATION REPORT NUMBER

9. SPONSORING/MONITORING AGENCY NAME(S) AND ADDRESS(ES)
Air Force Research Laboratory
Air Vehicles Directorate
Wright-Patterson Air Force Base, OH 45433-7542
Air Force Materiel Command
United States Air Force

10. SPONSORING/MONITORING AGENCY ACRONYM(S)
AFRL/RBAA

11. SPONSORING/MONITORING AGENCY REPORT NUMBER(S)
AFRL-RB-WP-TM-2010-3001

12. DISTRIBUTION/AVAILABILITY STATEMENT
Approved for public release; distribution unlimited.

13. SUPPLEMENTARY NOTES
PAO Case Number: 88ABW 2009-4237; Clearance Date: 30 Sep 2009. Report contains color.

14. ABSTRACT
A study of the transition behavior of the X-51 vehicle outer moldline has been made with particular emphasis on the leeward centerline of the vehicle. Based on encouraging earlier studies of first and second mode growth along the symmetry plane of other three-dimensional vehicle shapes, the focus of this work was to assess whether first or second mode growth is primarily responsible for transition along the leeward symmetry plane of the X-51.

The authors selected several test cases from the database of available wind tunnel tests where measurements of the position of transition on the leeward side of the body were obtained. A grid of the three-dimensional forebody shape of the vehicle was generated, mean flow analysis completed for all test cases and the solution symmetry plane was extracted for each case to compute a planar and oblique modal disturbance analysis. For each case, the growth of the most unstable disturbances was assessed to determine if the cause of transition could be attributed to modal disturbance growth for any or all of these cases.

15. SUBJECT TERMS
hypersonic transition, boundary layer transition, modal growth

16. SECURITY CLASSIFICATION OF:			17. LIMITATION OF ABSTRACT:	18. NUMBER OF PAGES	19a. NAME OF RESPONSIBLE PERSON (Monitor)
a. REPORT	b. ABSTRACT	c. THIS PAGE			Alyson Turri
Unclassified	Unclassified	Unclassified	SAR	20	19b. TELEPHONE NUMBER *(Include Area Code)* N/A

Standard Form 298 (Rev. 8-98)
Prescribed by ANSI Std. Z39-18

TABLE OF CONTENTS

LIST OF FIGURES

LIST OF TABLES

1 Introduction

A study of the transition behavior of the X-51 vehicle outer moldline (OML) has been made with particular emphasis on the leeward centerline of the vehicle. Based on encouraging earlier studies of first and second mode growth along the symmetry plane of other three-dimensional vehicle shapes, the focus of this work was to assess whether first or second mode growth is primarily responsible for transition along the leeward symmetry plane of the X-51.

The authors selected several test cases from the database of available wind tunnel tests where measurements of the position of transition on the leeward side of the body were obtained. A grid of the three-dimensional forebody shape of the vehicle was generated, mean flow analysis completed for all test cases and the solution symmetry plane was extracted for each case to compute a planar and oblique modal disturbance analysis. For each case, the growth of the most unstable disturbances was assessed to determine if the cause of transition could be attributed to modal disturbance growth for any or all of these cases.

2 Test Cases Selected for Study

The X-51 vehicle [1] is shown in Figure 1. The OML of the vehicle has been tested in several ground test facilities to characterize the transitional behavior and aerothermal loads for the flight test. The ground test databases include a 100% (full-scale) model tested in the CUBRC LENS-II facility [2], a 40% model tested in the LaRC Mach 6 facility [3], and 20% model tested in the Purdue BAM6QT facility [4]. From these activities, several cases were chosen with well-characterized transition measurements made using various techniques. At CUBRC, transition was measured using discrete thin-film heat transfer sensors. At LaRC, transition was detected using global phosphor thermography. At Purdue, measurements were made using temperature sensitive paint.

Figure 1. Artist Rendering of X-51 Vehicle and Booster

The conditions used for the cases selected for this analysis are shown in Table 1.

Table 1. Freestream Conditions for Ground Test Cases Selected for Modal Analysis Study

LaRC 40% Model Freestream Conditions							
Run	Mach	Re (1/m)	AoA (deg)	Twall (K)	T (K)	rho (kg/m^3)	P (N/m^2)
5	5.96	6.64E+06	4.00	300.0	62.5	0.0315	565.2
6	6.01	1.31E+07	4.01	300.0	62.0	0.0615	1092.5
7	6.03	1.83E+07	4.01	300.0	63.2	0.0865	1567.7
8	6.04	2.27E+07	4.02	300.0	62.8	0.1071	1927.2
9	6.04	2.26E+07	0.02	300.0	63.1	0.1069	1931.8
10	6.04	2.21E+07	2.02	300.0	63.6	0.1048	1910.4
11	6.04	2.23E+07	3.02	300.0	63.3	0.1055	1910.9
12	6.04	2.25E+07	4.98	300.0	63.3	0.1064	1928.0
13	6.04	2.27E+07	5.99	300.0	63.2	0.1073	1940.1
CUBRC Full-Scale Model Freestream Conditions							
Run	Mach	Re (1/m)	AoA (deg)	Twall (K)	T (K)	rho (kg/m^3)	P (N/m^2)
4	5.95	9.09E+06	4.00	296.0	212	0.0732	4472.0
5	5.94	4.63E+06	4.00	293.0	204	0.0367	2155.0
14	5.92	1.61E+07	4.00	297.0	234	0.1340	9060.00
Purdue 20% Model Freestream Conditions							
Run	Mach	Re (1/m)	AoA (deg)	Twall (K)	T (K)	rho (kg/m^3)	P (N/m^2)
	6	6.23E+06	4.00	300.0	55	0.0250	394.6

3 Grid Design

The challenge for this shape is the complexity of the grid topology required to properly resolve the surface. After studying the features of the vehicle including the inlet ramps, cowl integration, fins, etc., it was determined that only the front part of the vehicle should be gridded with emphasis on the leeward side of the vehicle and a minimum of grid points on the windward side. Because of the complexity and sharp corners of the inlet ramp geometry, it is not possible to adequately resolve this region without using an excessive number of grid points. For the leeward stability analysis, it was considered better to place those grid points on the leeward side rather than waste them on the inlet ramps.

The grids were generated with the software Gridgen. The final grids consisted of approximately 11-million cells with 150 points in the wall normal direction and 22-million cells with 300 points in the wall normal direction. The grid was loosely adapted to the shape of the bow shock to maximize the number of cells residing both within the shock layer and within the boundary layer. Several views of the final grid are shown in Figure 2.

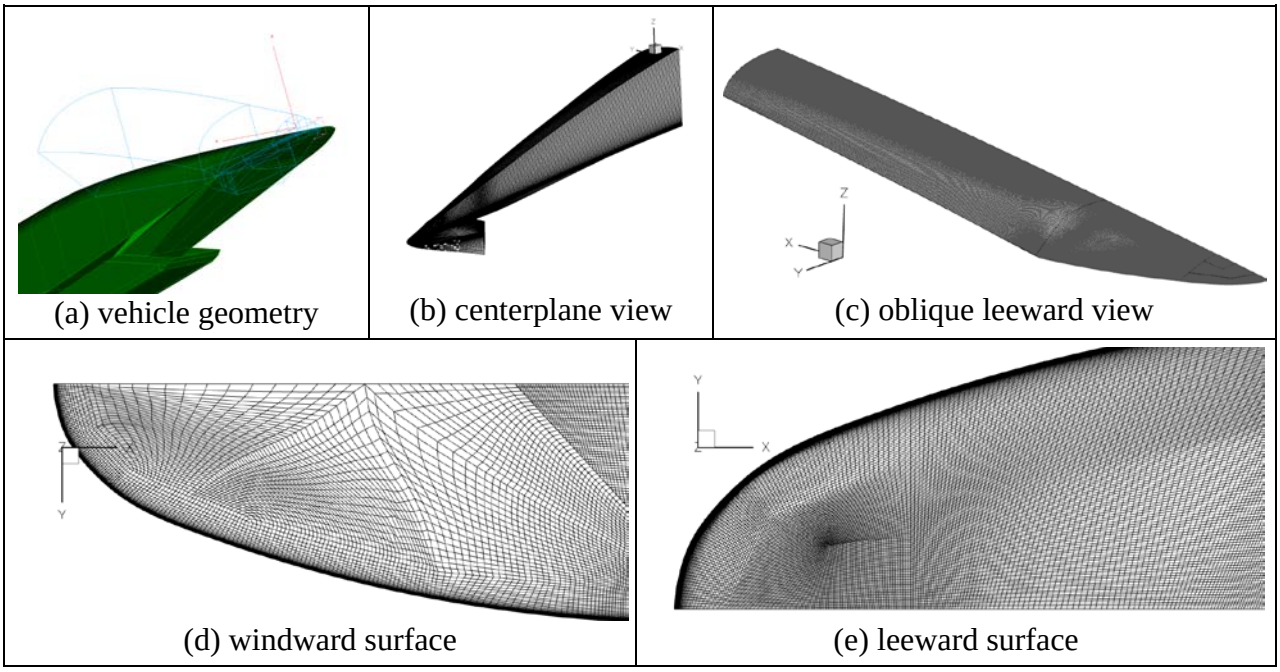

Figure 2. Several Views of Grid Developed for Leeward Stability Mean Flow Computations. The views in (d) and (e) are focused on the leading edge of the X-51 vehicle.

4 Mean Flow Solution

The grids with 11 and 22 million cells were run with the US3D unstructured mean flow solver [5], [6] assuming laminar flow. At Mach 6, the flow may be considered a perfect gas. Each run was completed using approximately 4000 timesteps at a global CFL of up to 12,000. Each case was completed in only a few hours. The laminar surface heat flux and pressure is shown for the Purdue case in Figure 3 as a typical example of the distribution on the leeward side in the region of interest. The centerplane of the finest grid for each case was extracted and transformed back to a single-block, structured format in order to perform the modal stability analysis.

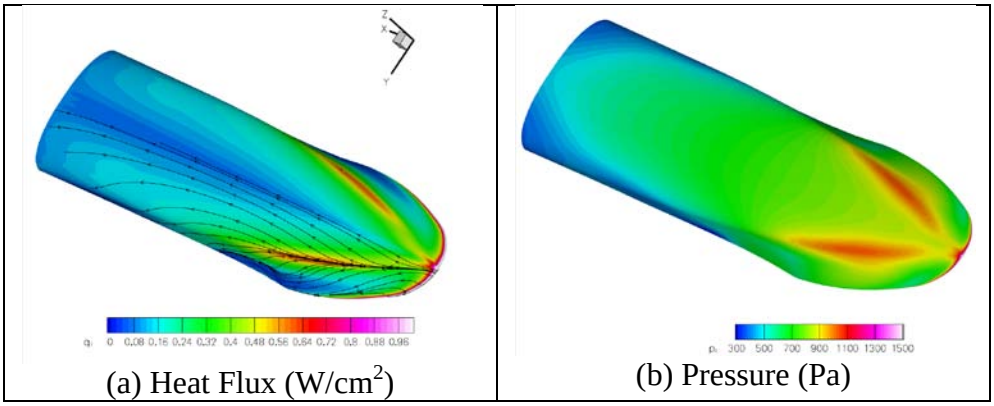

(a) Heat Flux (W/cm^2) (b) Pressure (Pa)

Figure 3. Mean Flow Surface Heat Flux and Pressure

5 Stability Solutions

The modal stability analysis was performed using the Stability and Transition Analysis for hypersonic Boundary Layers (STABL) code [7]-[9], which solves the parabolized stability equations (PSE) for two-dimensional or axisymmetric flows. The PSE equations are developed by modeling instantaneous flow variables of the Navier-Stokes equation set with a mean and fluctuating component and subtracting the mean component from the resulting equation set. The result is a system of 2nd order partial differential equations for the disturbances, which are parabolized according to the method of Herbert [10] by assuming that the disturbances are composed of a fast-oscillatory wave part and a slowly-varying shape function. The ellipticity of the wave part is preserved while only the governing equation for the shape function is parabolized. Assuming that initial disturbances are small and making an assumption of "locally-parallel" flow at the starting plane allows sufficient simplification to generate an initial solution for the shape function and complex streamwise wavenumber. These initial solutions may then be marched downstream to assess the growth or decay of each disturbance. The PSE analysis generates a prediction for the evolution of an initial disturbance as it moves downstream from its starting point through the mean flowfield. To predict the onset of transition, an experimental correlation is required. STABL uses the semi-empirical e^N correlation method. The N factor is defined as the log of the total amplitude growth of unstable boundary layer disturbances at particular frequencies [7]. Experimental studies have shown N to be about 8 – 11 for quiescent flight environments and levels around 5.5 (sometimes lower) for tunnel environments where freestream noise levels can be somewhat larger.

STABL is nearly automated with each case and the solution for the maximum disturbance growth envelope can be obtained for these conditions in about 30 minutes per case. The Purdue case is considered in detail before summarizing the results of the other cases studied.

The predicted second-mode planar instability growth is summarized as a function of position starting from the leading edge on the leeward centerplane of the 20% scale X-51 for the Purdue condition in Figure 4.

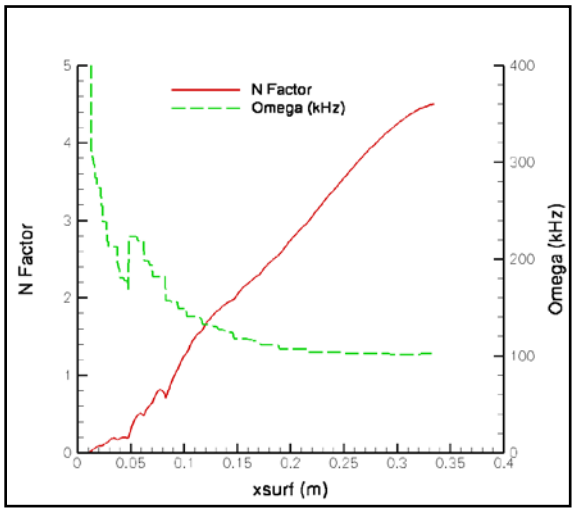

Figure 4. Disturbance N-factor Growth and Most Unstable Frequency of Planar Disturbances for Purdue Case

The right-hand axis of the plot shows the corresponding most unstable frequency that caused the peak N-factor at each station. In this result, the analysis was limited to planar waves only. The most unstable frequency does generally follow the empirical estimate for second-mode frequency, but the amplification reaches only to slightly less than 5.0 at the back end of the model. An amplification N-factor of 5.0 is close to the point where second mode may cause initial transition onset under noisy conditions, but not under quiet or flight conditions.

Because the cold flow conditions in the Purdue facility imply a very small ratio of wall to total temperature (which tends to stabilize second-mode disturbances), a second phase analysis was performed to look at oblique disturbances characteristic of first-mode transition. The stability diagram mapping relative growth through temporal and spanwise wave angle spectrums shows two regions of highest growth in Figure 5 – low spanwise wave angle (planar) instabilities at high frequency, and high spanwise wave angle (oblique) instabilities at low frequency.

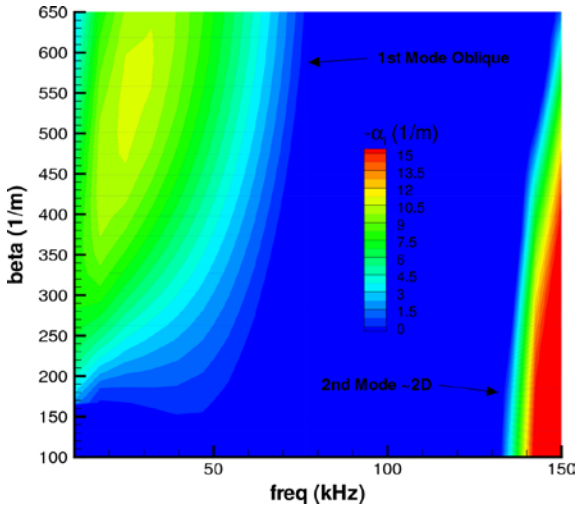

Figure 5. Stability Diagram Showing Regions of Oblique and Planar Wave Instability at s=0.1 m for Purdue Case

The centers of these regions are the first and second mode instabilities for the vehicle. When the N-factor is plotted as a function of station on the leeward centerplane as shown in Figure 6, the analysis shows that near the leading edge of the vehicle, the first mode is the most unstable with a spanwise wave angle near 70^{O}. At stations downstream of 0.15-m, the second-mode becomes most dominant and the wave angle drops to near zero. However, the maximum N-factor observed anywhere on the body is still the original value at the very back of the body. The N-factors attributed to first mode instability, while being larger than second mode near the leading edge, are still significantly too small to cause transition.

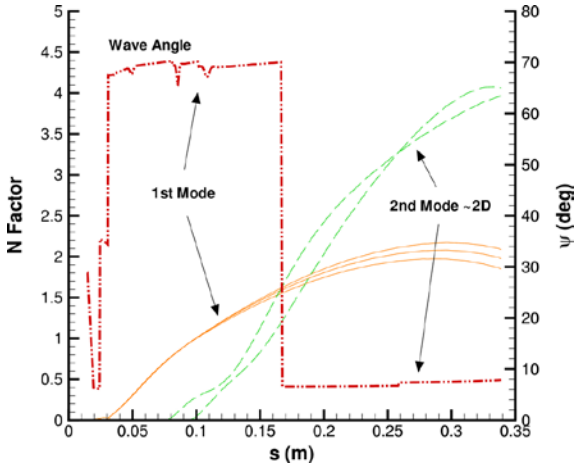

Figure 6. Disturbance N-factor Growth and Most Unstable Wave Angle of Mixed Oblique and Planar Disturbances for Purdue Case

The LaRC cases are considered in two phases because there are a large number of them. First, the trend with angle of attack of the vehicle is shown in Figure 7, which shows the predicted maximum N-factors for LaRC Runs 8 – 13 and the experimental data extracted from the phosphor images, where the sudden increase in non-dimensional heating may be attributed to transition. It should be noted that the experimental data covers only ¼ of the range of the N-factor graphic so the modal growth analysis predicts an N-factor of less than 1.0 for each case where the experimental data shows transition. The trend is correctly predicted by STABL, where an increase in angle of attack results in less modal growth and delayed transition because the leeward side of the body experiences larger expansion.

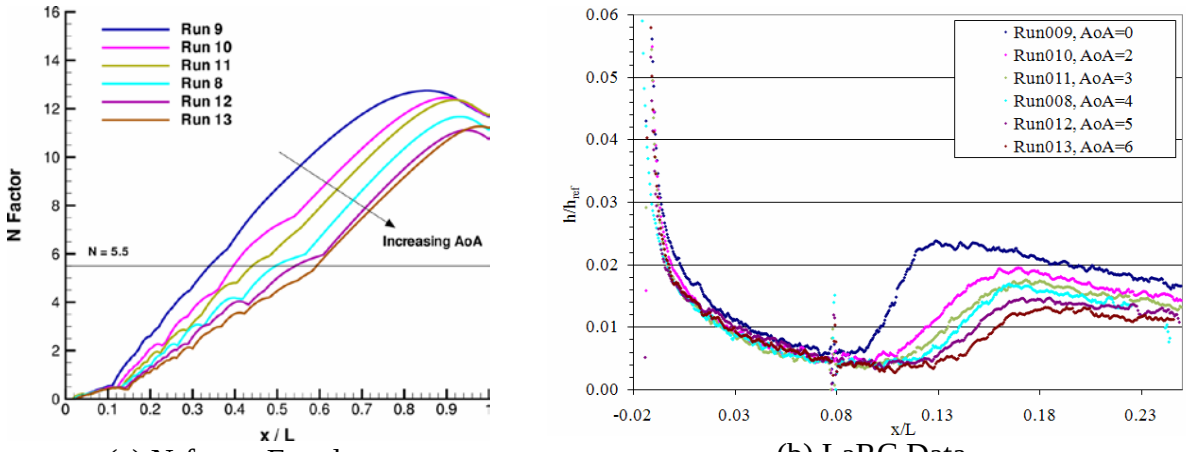

(a) N-factor Envelope (b) LaRC Data

Figure 7. Disturbance N-factor Growth and LaRC Data Showing Transition Onset for Several Cases varying Angle of Attack at an Approximate Freestream Reynolds Number of 22 million per meter. The spike in (b) is a fiducial mark and not a trip. (L ≈ 0.67 m)

The trend with Reynolds number is also shown in Figure 8, which shows the predicted maximum N-factors for LaRC Runs 5 – 8 at a constant angle of attack of 4.0^{O}. Although the lowest Reynolds number condition does not show clear evidence of transition in the experimental data, the other three Reynolds numbers show transition onset occurs where the N-factor is less than or equal to about 1.0. Again the correct trend is captured for this case by the STABL code, but the magnitude of growth is far too small to be primarily responsible for the transition onset observed in the runs.

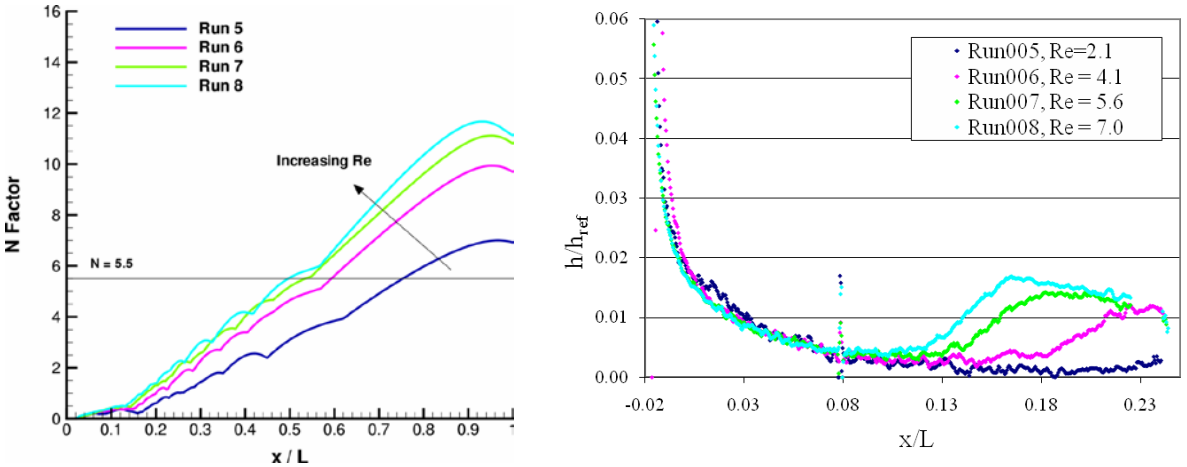

(a) N-factor Envelope (b) LaRC Data

Figure 8. Disturbance N-factor Growth and LaRC Data Showing Transition Onset for Several Cases varying Freestream Unit Reynolds Number. The spike in (b) is a fiducial mark and not a trip. (L ≈ 0.67 m)

Finally, the three CUBRC cases are considered on a full-scale body. These cases are also the only ones to replicate the total enthalpy of the flight in the test. The summary of the predicted maximum N-factor growth and the experimental data are shown in Figure 10. Here, the result is similar to the previous conclusion from the LaRC comparisons. For all three CUBRC cases transition occurs very far forward within the first 24" on the model. The predicted N-factor for second mode growth is far less than 1.0 for each case. Finally, as before, an oblique wave analysis was performed for the CUBRC Run 4 case to verify that no additional growth would be seen from first-mode activity since transition occurs so close to the leading edge. This result is shown in Figure 9, which demonstrates that, although the oblique wave disturbance envelope is slightly larger than the planar one, the levels are still insignificant for all modal waves. Although the N factors are very low, it is expected to be a highly unstable boundary layer due to the converging flow on the centerline as seen in Figure 3a. This highlights the deficiencies of analyzing a highly three-dimensional flow with a two-dimensional stability solver.

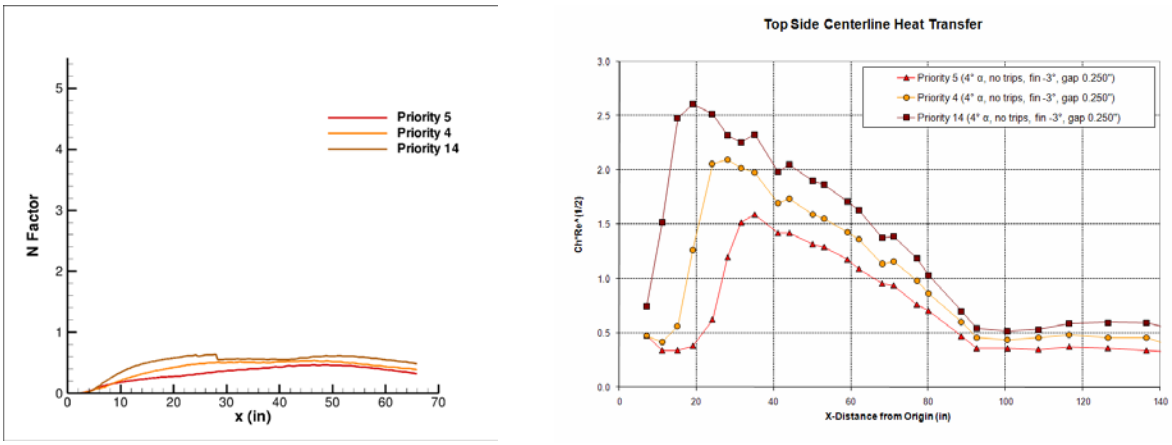

(a) N-factor Envelope (b) CUBRC Data

Figure 9. Disturbance N-factor Growth and CUBRC Data Showing Transition Onset for Several Cases varying Freestream Unit Reynolds Number (4 – 9.09E+06 m^{-1}, 5 – 4.63E+06 m^{-1}, 14 – 1.61E+07 m^{-1})

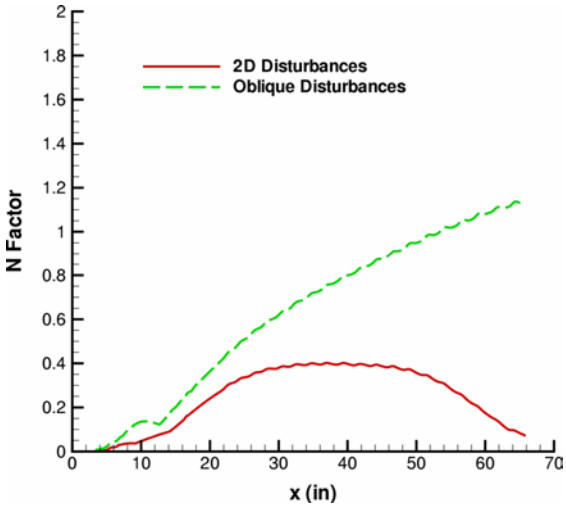

Figure 10. Disturbance N-factor for Mixed Oblique and Planar Disturbances for CUBRC Run 4

6 Conclusions

After analyzing thirteen different cases from three ground test facilities, it has been concluded that the most likely dominant transition mechanism for the leeward side of the X-51 will be crossflow. There is experimental evidence from LaRC and CUBRC tests to support this conclusion which show a rise in heat transfer occurring outboard near the swept leading edge and propagating inward toward the centerline. The only test case to show any significant N-factor growth on the leeward centerplane was the Purdue case. Although the most unstable disturbances did not amplify enough to cause likely natural transition in a quiescent environment, the N-factors obtained were non-negligible and a detailed analysis of the crossflow modes of stability need to be performed for this case to determine the relative importance of modal growth. An analysis of crossflow should be made for all conditions studied here to verify the conclusions of this study, but we have seen little evidence to suspect that any significant modal growth will be experienced on the leeward side of X-51 for real flight conditions.

7 References

[1] Wikipedia. <http://en.wikipedia.org/wiki/Boeing_X-51>. Accessed 14 July 2009.

[2] Matthew MacLean, "MacLean_summer_study_2008-10-27.ppt", unpublished data, NASA Langley Research Center Aerocompass Collaborative Data Exchange Site <http://aerocompass.larc.nasa.gov/>.

[3] Karen Berger, "T6948_Run_Matrix_final.xls", unpublished data, NASA Langley Research Center Aerocompass Collaborative Data Exchange Site <http://aerocompass.larc.nasa.gov/>.

[4] Borg, M., Schneider, S., "Effect of Freestream Noise on Instability and Transition for the X-51A Lee Side," AIAA Paper No. 2009-0396, 47th AIAA Aerospace Sciences Meeting including The New Horizons Forum and Aerospace Exposition, Orlando, FL. January 2009.

[5] Nompelis, I., Drayna, T. W., and Candler, G. V., "A Parallel Unstructured Implicit Solver for Hypersonic Reacting Flow Simulation," AIAA Paper No. 2005-4867, June 2005.

[6] Nompelis, I., Wan, T., and Candler, G. V., " Performance Comparisons of Parallel Implicit Solvers for Hypersonic Flow Computations on Unstructured Meshes," AIAA Paper No. 2007-4334, June 2007.

[7] Johnson, Heath B. *Thermochemical Interactions in Hypersonic Boundary Layer Stability*. Ph.D. Thesis, University of Minnesota, Minneapolis, MN, 2000.

[8] Johnson, H. and Candler, G. "Hypersonic Boundary Layer Stability Analysis Using PSE-Chem." AIAA Paper 2005-5023. 35TH AIAA Fluid Dynamics Conference and Exhibit, Toronto, ON. June 2005.

[9] Johnson, H. and Candler, G. "Analysis of Laminar-Turbulent Transition in Hypersonic Flight Using PSE-Chem." AIAA Paper 2006-3057. 36TH AIAA Fluid Dynamics Conference and Exhibit, San Francisco, CA. 5 – 8 June 2006

[10] Herbert, T. "Boundary Layer Transition – Analysis and Prediction Revisited." AIAA Paper 91-0737. January, 1991.